The formation of double-row oxide stripes during the initial oxidation of NiAl(100)

Hailang Qin and Guangwen Zhou

Citation: J. Appl. Phys. **114**, 083513 (2013); doi: 10.1063/1.4819759
View online: http://dx.doi.org/10.1063/1.4819759
View Table of Contents: http://jap.aip.org/resource/1/JAPIAU/v114/i8
Published by the AIP Publishing LLC.

The formation of double-row oxide stripes during the initial oxidation of NiAl(100)

Hailang Qin and Guangwen Zhou[a)]
Department of Mechanical Engineering and Multidisciplinary Program in Materials Science and Engineering, State University of New York, Binghamton, New York 13902, USA

(Received 21 July 2013; accepted 13 August 2013; published online 27 August 2013)

The initial growth of ultrathin aluminum oxide film during the oxidation of NiAl(100) was studied with scanning tunneling microscopy. Our observations reveal that the oxide film grows initially as pairs of a double-row stripe structure with a lateral size equal to the unit cell of θ-Al_2O_3. These double-row stripes serve as the very basic stable building units of the ordered oxide phase for growing thicker bulk-oxide-like thin films. It is shown that the electronic properties of these ultrathin double-row stripes do not differ significantly from that of the clean NiAl surface; however, the thicker oxide stripes show a decreased conductivity. © *2013 AIP Publishing LLC*. [http://dx.doi.org/10.1063/1.4819759]

I. INTRODUCTION

The formation of ultrathin aluminum oxide films on the NiAl intermetallic alloys has been extensively studied owing to its significant practical importance in high-temperature protective coatings, and catalyst supports due to the inertness and chemical stability of the aluminum oxide film.[1–10] The thin oxide can be formed by exposing the alloy surface to oxygen gas either at room temperature followed by high temperature annealing or oxygen dosing directly at high temperature. The structures of these oxides have been determined by electron energy loss spectroscopy, low energy electron diffraction (LEED), scanning tunneling microscopy (STM), and low energy electron microscopy (LEEM).[11–20] Blum *et al.*[12,13] showed that oxide stripes can form along ⟨001⟩ and ⟨010⟩ directions of the NiAl(100) surface and the stripes have a mean width of about 27 Å and a height of 3 Å or larger. Maurice *et al.*[15] observed high resolution STM images on the oxides grown on NiAl(100) that are in agreement with the surface structure of the θ-Al_2O_3 phase.

In this work we present STM and scanning tunneling spectroscopy (STS) studies of the initial oxidation of NiAl(100). It is shown that the oxide stripes grow actually as isolated pairs of a double-row stripe structure in the early stage. The spacing between the two rows is about 6 Å, and the height of these stripes is only about 0.8–1.0 Å, which is much smaller than what has been reported in the literature.[12,18] Furthermore, the spacing between two double-row stripes varies and can be as small as 22 Å, which is about the spacing for another double-row stripe to grow in between. All the evidence suggests that the observed double-row stripe structure is the basic building unit of the ordered oxide phase for the growth of the bulk-oxide-like (2×1) superstructure of the θ-Al_2O_3 film on NiAl(100). The STS measurements show that the electronic properties of these ultrathin double-row stripes do not differ significantly from that of the clean NiAl surface, while the co-existing thicker stripes of about 3 Å thick exhibit a clear decreased conductivity.

II. EXPERIMENT

All the experiments were performed in an ultrahigh vacuum (UHV) chamber equipped with an ion sputter gun, LEED, and Auger electron spectroscopy. The base pressure in the STM chamber was about 1.0×10^{-10} Torr. The single-crystal NiAl(100) substrate has an orientation accuracy better than 0.1° to the (100) crystallographic orientation. The sample was first cleaned by cycles of Ar^+ ion sputtering (1 keV, 2 μA) for 20 min at room temperature and subsequent annealing at about 850 °C for 10 min. Finally, the sample was annealed at 700 °C for 3 h to produce a well-defined $c(3\sqrt{2} \times \sqrt{2}, \sqrt{2} \times 3\sqrt{2})R45°$ superstructure, as checked by LEED.[14,15] The oxidation was performed by exposing the clean NiAl(100) sample to gaseous oxygen at room temperature followed by annealing at 750 °C for 4 h. The oxides studied were grown at the oxygen exposures of 1 Langmuir (L, $1\,L = 10^{-6}$ Torr·s) and 10 L, respectively. The STM measurements were performed at room temperature with a mechanically cut PtIr tip using a UHV 750 (RHK Technology, Inc.) system. The STM images were acquired at constant-current mode with the bias on the sample.

III. RESULTS AND DISCUSSIONS

Figure 1(a) is a typical STM image of the oxide formed by exposing the clean NiAl(100) surface to oxygen gas at the pressure of 1.0×10^{-8} Torr for 100 s (1 L) at room temperature. The surface exhibits the feature of an amorphous oxide film, which is consistent with other reported studies.[13] In addition, there are no clear isolated oxide islands on the terrace or near the step edge. This indicates that the amorphous oxide growth at room temperature is relatively uniform. The sample was then annealed at 750 °C for 4 h to form an ordered alumina layer, as shown in Figure 1(b). The resulting surface presents two major types of areas. The first type (denoted by (1) in Figure 1(b)) is covered by a well-

a)Author to whom correspondence should be addressed. Electronic mail: gzhou@binghamton.edu

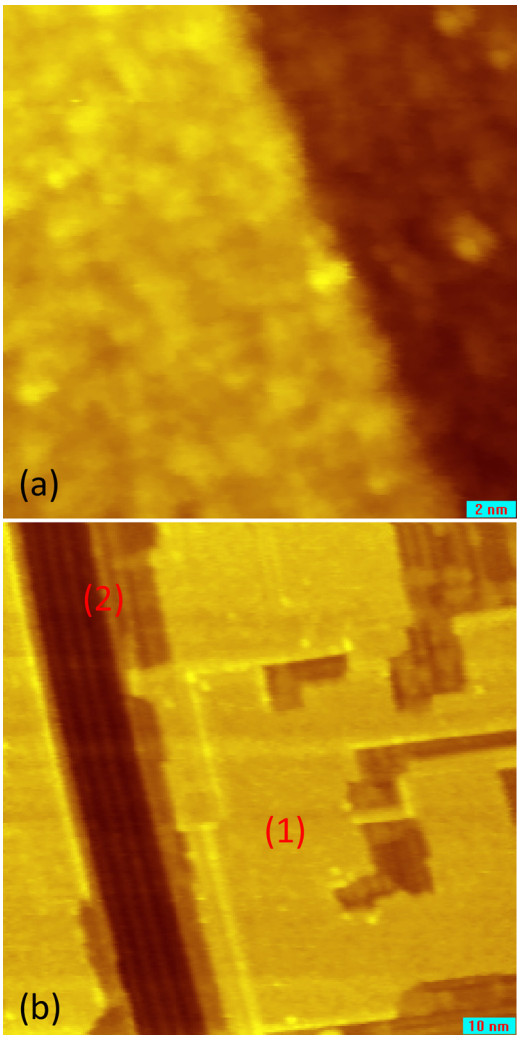

FIG. 1. STM images ($V_{Bias} = -1$ V, $I_t = 0.5$ nA) of the NiAl(100) surface after 1 L oxygen exposure at room temperature (a) before (21×21 nm^2, color scale: 0.5 nm) and (b) after (100×100 nm^2, color scale: 0.7 nm) annealing. Labels of (1) and (2) indicate the two regions described in the text.

crystallized oxide layer with a thickness of about 3.0 Å, and the other type (denoted by (2) in Figure 1(b)) consists of oxide stripes propagating along ⟨010⟩ and ⟨001⟩ directions. These stripes have different heights, and the smallest one shows a double-row stripe structure with a height of only about 0.8–1.0 Å (Note: The height value remains the same when the line profile is drawn perpendicular to the stripes), as will be discussed below. These double-row stripes can also be observed at the edges of or even within the first type of area.

A close-up view of the upper left corner of Figure 1(b) is shown in Figure 2(a). As can be seen, each thin stripe in Figure 1(b) actually consists of two small stripes (a double-row stripe structure). The spacing between the two rows is about 6 Å (note that the spacing was actually measured by drawing the line profile perpendicular to the stripes). The height of the rows is only about 1.0 Å as shown in Figure 2(b), which is much smaller than what has been observed by others.[12] Furthermore, the spacing between two double-row stripes varies and can be as small as 22 Å, which is about the spacing for another double-row stripe to grow in between, as illustrated in Fig. 2(c). This is also shown by the thick red lines drawn in Fig. 2(a).

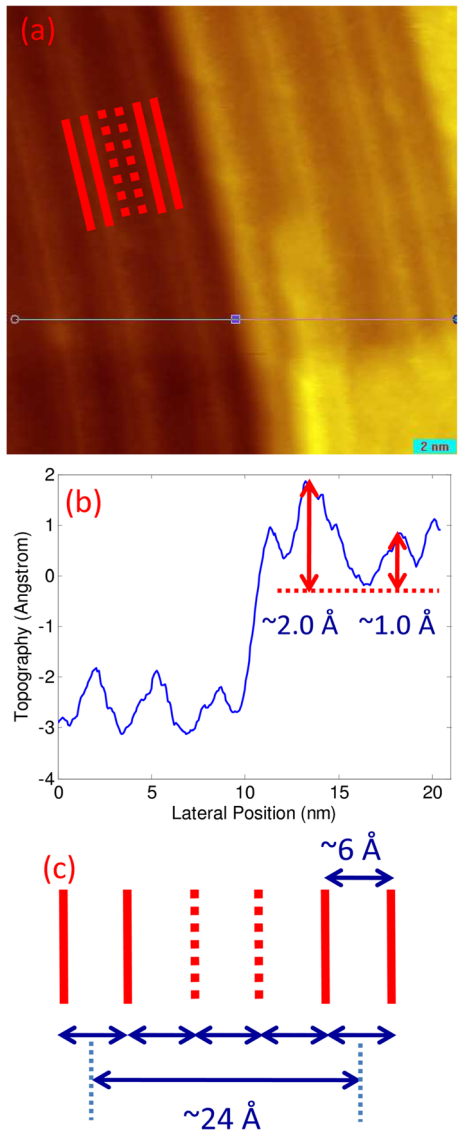

FIG. 2. (a) STM image (21×21 nm^2, $V_{Bias} = -1$ V, $I_t = 1$ nA, color scale: 0.7 nm) of the NiAl(100) surface after 1 L oxygen exposure at room temperature and subsequent annealing at 750 °C for 4 h. The thick red lines along the stripes are for illustration only. (b) A line profile of the lateral line drawn in (a). The two double arrows indicate a double-row stripe structure and a thicker stripe. (c) Illustration showing the spacing required for growing another double-row stripe (dotted red line) between two existing double-row stripes (solid red line).

The same double-row stripe structure is also observed on the surface oxidized by oxygen exposure of 10 L at the partial pressure of 1.0×10^{-7} Torr and subsequently annealing at 750 °C for 4 h, as shown in Figures 3(a) and 3(b). The spacing between the two thin rows is about 6 Å, and the smallest spacing between two double-row stripes is about 22 Å. The height of the double-row stripes is measured to be about 0.8 Å, which is close to the one observed on the oxide formed with 1 L oxygen exposure. It should be noted that the measured heights of the oxide stripes can vary with the bias voltage,[18,20] but it is also found that the height is largely independent of the bias measured in our experiments ranging from −0.5 V to −1.0 V. The double-row stripes are formed from the high-temperature annealing at 750 °C under vacuum, which suggests that these fine stripes represent an ordered and stable oxide phase.

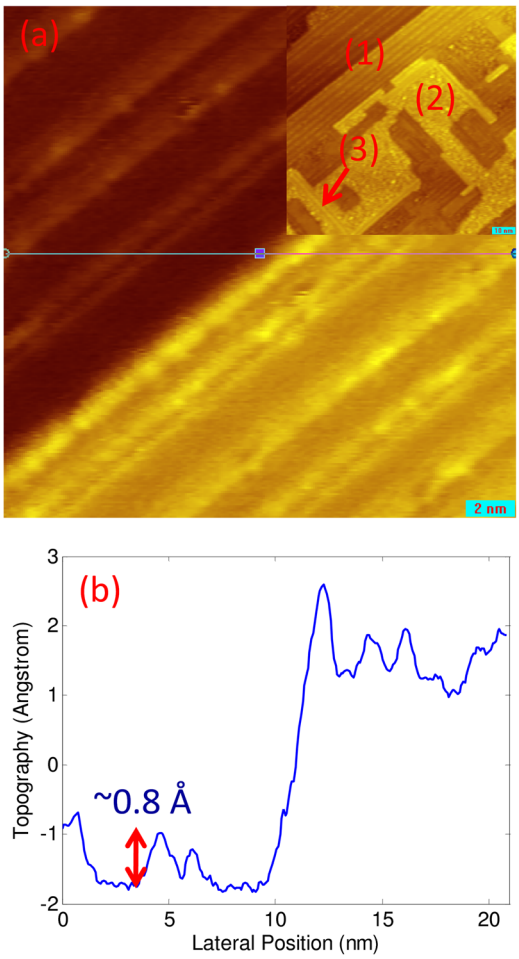

FIG. 3. STM image (21×21 nm^2, $V_{Bias} = -1$ V, $I_t = 1$ nA, color scale: 1.0 nm) of the NiAl(100) surface after 10 L oxygen exposure at room temperature and subsequent annealing at 750 °C for 4 h (b) The line profile of the lateral line drawn in (a). The inset in (a) is an image (100×100 nm^2, $V_{Bias} = -1$ V, $I_t = 1$ nA, color scale: 1.0 nm) of a larger area that includes (a). The regions with labels of (1), (2), and (3) are thin-stripe, amorphous-oxide, and thick-stripe areas, respectively.

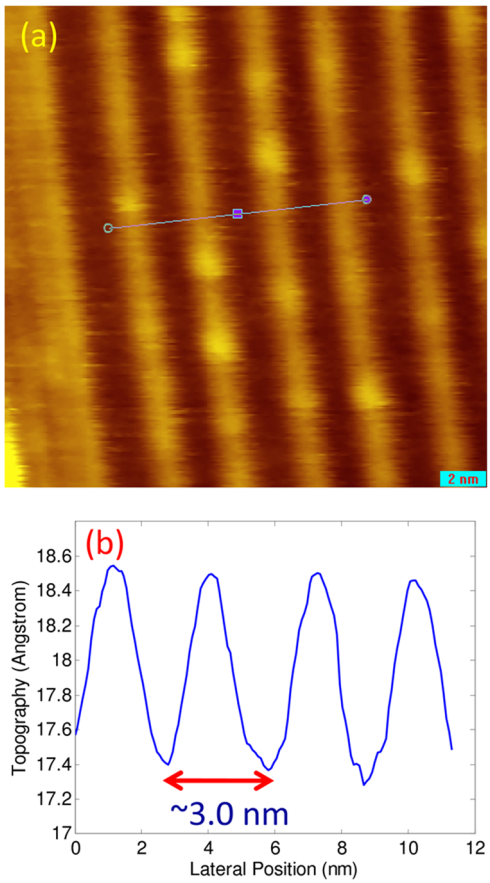

FIG. 4. (a) STM image (21×21 nm^2, $V_{Bias} = -1$ V, $I_t = 1$ nA, color scale: 0.3 nm) of oxide stripes on NiAl(100) oxidized and annealed at 750 °C; (b) The corresponding line profile of the line drawn in (a).

The formation of oxide stripes was also observed by oxidizing a clean NiAl(100) surface directly at a high temperature, but their structure features are found to be different from the results described above. As an example, Fig. 4(a) shows a STM image of the oxide stripes formed on the NiAl(100) surface oxidized at 750 °C followed by vacuum annealing at the same temperature. Fig. 4(b) is a line profile obtained from the line drawn in Fig. 4(a). It can be seen that the stripe spacing is about 3 nm and the stripe height is about 1.2 Å. These observations are consistent with the earlier studies under the similar oxidation condition, and more details can be found from the results by Hsu *et al.*[18] The stripe spacing of 3 nm is much larger than that (i.e., stripe spacing of 6 Å) for oxide stripes formed by first oxidizing the NiAl(100) at room temperature followed by vacuum annealing at 750 °C. In addition, the double-row stripes observed here from the room-temperature oxidation followed by annealing at 750 °C are surrounded by clean surface areas, instead of oxide domains that Hsu *et al.*[18] observed from the oxidation at the high temperature. This is further supported by the LEED pattern as shown in Fig. 5(a) and its schematic in Fig. 5(b). The LEED pattern was taken on a sample oxidized by oxygen exposure of 10 L with the partial pressure of 1×10^{-7} Torr at room temperature and subsequently annealed at 750 °C for 4 h. The LEED pattern shows the $(2 \times 1, 1 \times 2)$ superstructure of the oxide with streaks. In addition, it shows the $c(3\sqrt{2} \times \sqrt{2}, \sqrt{2} \times 3\sqrt{2})R45°$ surface reconstruction of the clean surface.[14,15] This suggests that the surface was not fully covered by the oxides; some clean surface areas like the region between two double-row stripes was still not oxidized.

The oxide formed from the oxidation was usually assigned to θ-Al_2O_3, which has a monoclinic lattice with parameters of a = 5.64 Å, b = 2.92 Å, c = 11.83 Å, and $\alpha = 104°$.[11] The spacing of 6 Å between the two thin rows is very close to the *a* parameter of a single unit cell of the bulk θ-Al_2O_3 structure along the [100] direction. It is also in agreement with a spacing of 2×2.89 Å perpendicular to the stripes in the (2×1) superstructure observed in the LEED pattern, in which the [010] direction of the θ-Al_2O_3 is parallel to the [100] direction of the NiAl ($2a_{NiAl} = 5.78$ Å, $a_{\theta-Al_2O_3} = 5.64$ Å) and the [010] direction of the θ-Al_2O_3 is parallel to the [001] direction of the NiAl ($a_{NiAl} = 2.89$Å, $a_{\theta-Al_2O_3} = 2.92$Å).[11,12] This suggests that the observed double-row stripe structure is a very basic structure unit (i.e., with a lateral size equal to one unit cell of θ-Al_2O_3) of the ordered oxide phase for the growth of thicker and wider oxide stripes on NiAl(100) and corresponds to the onset of the

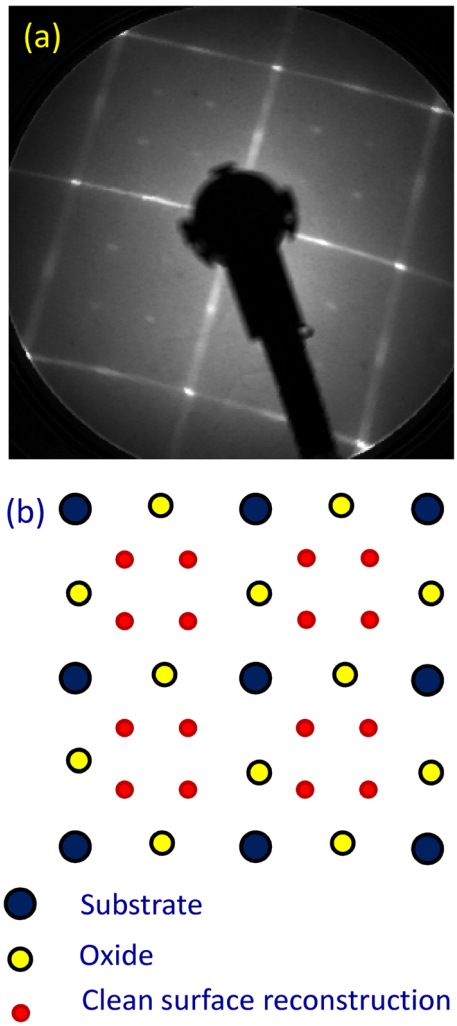

FIG. 5. (a) LEED pattern ($E_P = 111$ eV) of the NiAl(100) oxidized at oxygen pressure of 1×10^{-7} Torr at room temperature and annealed at 750 °C for 4 h. (b) The schematic of the corresponding LEED pattern in (a) shows the (1×1) substrate, the $c(3\sqrt{2} \times \sqrt{2}, \sqrt{2} \times 3\sqrt{2})R45°$ reconstruction on the clean surface, and the $(2 \times 1, 1 \times 2)$ oxide superstructure with streaks. The streaks are not shown in the schematic.

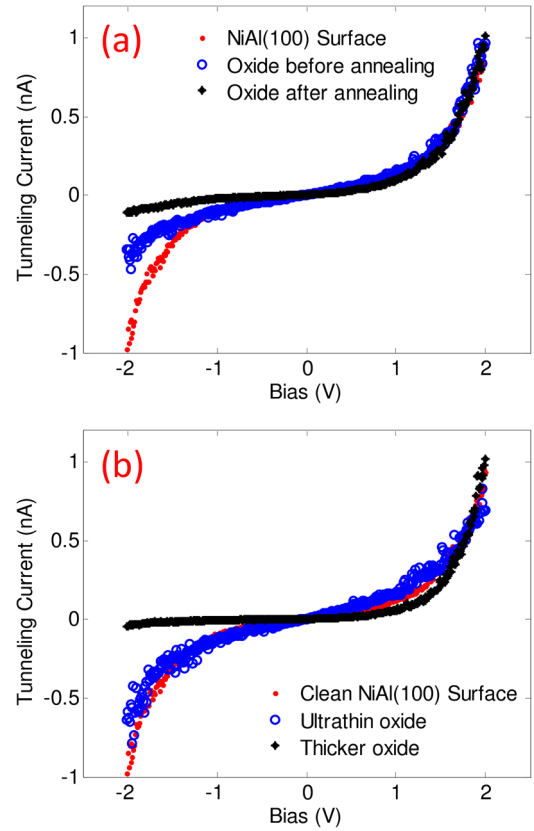

FIG. 6. STS acquired on (a) the clean surface, the oxide surface before annealing, and after annealing; (b) the clean surface, ultrathin and thicker oxide areas, respectively. Setpoint: $V_{Bias} = 2$ V, $I_t = 1$ nA.

formations of the bulk-oxide-like (2×1) superstructure of the θ-Al_2O_3 phase on the NiAl surface. The oxygen sublattice of θ-Al_2O_3 has a face-centered-cubic (fcc) structure with the lattice constant of 5.64 Å.[11] The measured row-spacing of 6 Å suggests that the double-row stripe structure is closely related to the lateral size of one unit cell of the oxygen sub-lattice.[11] The observed stripe height of only 0.8–1.0 Å indicates that the double-row stripes contain only one layer of oxygen atoms. With more oxygen layers grown on top and aluminum atoms added in the tetrahedral or octahedral sites, the stripes grow thicker.

The electronic properties of the thin oxide stripes were characterized with STS and compared with the thicker oxides. The STS was performed without the lock-in pre-amplifier and the post-processing differential STS spectra showed too much noise. Hence, the differential STS spectra were not shown. Figure 6(a) shows the representative spectra acquired on the clean NiAl(100) surface, the amorphous oxide film formed after 10 L oxygen exposure at room temperature, and the crystallized oxide surface (thickness of about 3 Å) formed by annealing the amorphous oxide film. There is a clear trend of decreasing conductivity for the clean NiAl surface, amorphous oxide film, and the ordered oxide film. The amorphous oxide film was relatively uniform before annealing. Structural ordering occurred upon high temperature annealing, which results in different types of surface areas: flat crystallized area, oxide stripe area, and sometimes still some amorphous area, as shown in Fig. 1(b) and the inset of Fig. 3(a). These areas exhibit different thicknesses, with the oxide stripe areas usually being thinner than the flat crystallized and amorphous areas. For the two oxidation conditions studied here, it was found that the thicker area is usually about 3 Å, while the stripe thickness in the stripe area varies from 0.8 Å for the double-row stripes to 3 Å for the thicker and wider stripes. The amorphous oxide thickness was expected to be less than 3 Å, and this is likely the reason why its conductivity was higher than the thicker oxide area, where the oxide was about 3 Å.

It is particularly interesting to compare the electronic properties of the double-row structure and the thicker and wider (2×1) oxide stripes since the former is believed to be the onset of the formation of the thicker oxide phase. Figure 6(b) shows three STS spectra taken from the clean NiAl surface, double-row stripes (ultrathin oxide film), and the thicker (2×1) oxide film, all from the surface oxidized with 1 L oxygen exposure followed by annealing 750 °C. The thicker oxide shows a significantly less conductivity compared with that of the clean surface, which is also consistent

with Figure 6(a). For the double-row stripe, however, there was no clear decrease in conductivity compared with the clean surface area. This is expected, considering that the thickness of the double-row stripe is only about 0.8–1.0 Å.

IV. CONCLUSION

In conclusion, the structure and the electronic properties of the oxide films grown on the single-crystal NiAl(100) substrate are investigated using scanning tunneling microscopy and spectroscopy. It is shown that the oxide grows initially as a double-row stripe structure. The double-row stripe consists of two small rows with a spacing of about 6 Å and a height of about 0.8–1.0 Å. It is suggested that this double-row stripe structure represents the basic stable structure unit of the ordered oxide phase on the NiAl(100) substrate and is the onset of the formations of the thicker stripes of the bulk-oxide-like θ-Al_2O_3. While the thicker (3 Å) oxide film shows a clear decrease in conductivity compared with the clean surface, the electronic properties of these ultrathin double-row stripes show no significant difference from that of the clean NiAl surface.

ACKNOWLEDGMENTS

This work was supported by the National Science Foundation under the Grant No. CBET-0932814.

[1]D. R. Mullins and S. H. Overbury, Surf. Sci. **199**, 141 (1988).
[2]N. Frémy, V. Maurice, and P. Marcus, Surf. Interface Anal. **34**, 519 (2002).
[3]P. Gassmann, R. Franchy, and H. Ibach, J. Electron. Spectrosc. Relat. Phenom. **64/65**, 315 (1993).
[4]A. Stierle, V. Formoso, F. Comin, and R. Franchy, Surf. Sci. **467**, 85 (2000).
[5]J. Méndez and H. Niehus, Appl. Surf. Sci. **142**, 152 (1999).
[6]W.-C. Lin, C.-C. Kuo, M.-F. Luo, K.-J. Song, and M.-T. Lin, Appl. Phys. Lett. **86**, 043105 (2005).
[7]M. F. Luo, C. I. Chiang, H. W. Shiu, S. D. Sartale, and C. C. Kuo, Nanotechnology **17**, 360 (2006).
[8]M. S. Zei, C. S. Lin, W. H. Wei, C. I. Chiang, and M. F. Luo, Surf. Sci. **600**, 1942 (2006).
[9]M. F. Luo, W. H. Wen, C. S. Lin, C. I. Chiang, S. D. Sartale, and M. S. Zei, Surf. Sci. **601**, 2139 (2007).
[10]C. T. Wang, C. W. Lin, C. L. Hsia, B. W. Chang, and M. F. Luo, Thin Solid Films **520**, 3952 (2012).
[11]P. Gassmann, R. Franchy, and H. Ibach, Surf. Sci. **319**, 95 (1994).
[12]R.-P. Blum, D. Ahlbehrendt, and H. Niehus, Surf. Sci. **396**, 176 (1998).
[13]R.-P. Blum and H. Niehus, Appl. Phys. A **66**, S529 (1998).
[14]N. Frémy, V. Maurice, and P. Marcus, J. Am. Ceram. Soc. **86**, 669 (2003).
[15]V. Maurice, N. Frémy, and P. Marcus, Surf. Sci. **581**, 88 (2005).
[16]W.-C. Lin, S.-S. Wong, P.-C. Huang, C.-B. Wu, B.-R. Xu, C.-T. Chiang, H.-Y. Yen, and M.-T. Lin, Appl. Phys. Lett. **89**, 153111 (2006).
[17]W.-C. Lin, P.-C. Huang, K.-J. Song, and M.-T. Lin, Appl. Phys. Lett. **88**, 153117 (2006).
[18]P.-J. Hsu, C.-B. Wu, H.-Y. Yen, S.-S. Wong, W.-C. Lin, and M.-T. Lin, Appl. Phys. Lett. **93**, 143104 (2008).
[19]K. F. McCarty, Surf. Sci. **474**, L165 (2001).
[20]J. P. Pierce and K. F. McCarty, Phys. Rev. B **71**, 125428 (2005).